Kinetics of Cold-Cap Reactions for Vitrification of Nuclear Waste Glass Based on Simultaneous Differential Scanning Calorimetry -Thermogravimetry (DSC-TGA) and Evolved Gas Analysis (EGA) – 14517

Carmen Rodriguez *, Jaehun Chun *, David Pierce *, Michael Schweiger *, Pavel Hrma *
* Pacific Northwest National Laboratory

ABSTRACT

For vitrifying nuclear waste glass, the feed, a mixture of waste with glass-forming and modifying additives, is charged onto the cold cap that covers 90–100% of the melt surface. The cold cap consists of a layer of reacting molten glass floating on the surface of the melt in an all-electric, continuous glass melter. As the feed moves through the cold cap, it undergoes chemical reactions and phase transitions through which it is converted to molten glass that moves from the cold cap into the melt pool. The process involves a series of reactions that generate multiple gases, and subsequent mass loss and foaming significantly influence the mass and heat transfers. The rate of glass melting, which is greatly influenced by mass and heat transfers, affects the vitrification process and the efficiency of the immobilization of nuclear waste. The cold-cap reactions of a representative waste glass feed were studied using both simultaneous differential scanning calorimetry–thermogravimetry (DSC-TGA) and thermogravimetry coupled with gas chromatography-mass spectrometry (TGA-GC-MS) as complementary tools to perform evolved gas analysis (EGA). Analyses from DSC-TGA and EGA on the cold-cap reactions provide a key element for the development of an advanced cold-cap model. It also helps to formulate melter feeds for higher production rates.

INTRODUCTION

The cost and schedule of high-level waste (HLW) treatment is highly dependent on the loading of HLW in glass and on the rate of HLW glass production. In a continuously fed glass melter, the rate of processing is jointly controlled by the rate of heat transfer from molten glass to the cold cap and by the kinetics of various chemical reactions and phase transitions within the cold cap [1-3]. The cold cap is a mixture of low-melting salts, glass-forming melts, undissolved refractory solids (sometimes in clusters), and various gases [4].

Inside the cold cap, the conversion of dry feed to glass takes places at around 1100°C as it moves towards the glass molten surface. This process spans the formation of molten salts that react with feed solids, turning them into intermediate products and ultimately the glass-forming melt. Various cold-cap reactions evolve gases that escape from the cold cap through open pores and through the bottom foam layer that develops beneath the cold cap [5]. Understanding the cold-cap reactions over the temperature range of the conversion process helps formulate melter feeds for higher production rate, and hence an enhanced efficiency of the vitrification facility.

Gas-evolving cold-cap reactions release chemically bonded water and produce NO_x, O_2, and CO_x from reactions of nitrates with organics and reactions of nitrates, nitrites and carbonates with solids [8-20]. Pokorny et al. [7] modeled the kinetics of the gas–evolving cold-cap reactions using data from non-isothermal TGA. Their model describes the overall reaction rate as a sum of mutually independent n^{th} order reaction kinetics with the Arrhenius rate coefficients. For simplification, they neglected interactions between consecutive reactions and the complex responses of multicomponent molten salts and reactants.

For the differential scanning calorimetry–thermogravimetry (DSC-TGA) study, the run/rerun method was utilized to separate the reaction heat from both the heat associated with the heat capacity of the feed and experimental artifacts. Calculating the degree of conversion based on the reaction heat, an n^{th} order kinetic model was applied, where the kinetic parameters were obtained using the Kissinger method, combined with least squares analysis. Furthermore, the heat capacity of the reacting feed was estimated from this analysis. The combination of thermogravimetry with gas chromatography-mass spectrometry (TGA-GC-MS) was used to perform qualitative and quantitative EGA for the cold-cap reactions, allowing the identification of gases released and the determination of their amounts as a function of temperature while the sample is subjected to a controlled temperature program. Previous informative, yet semi-quantitative, EGA studies analyzed off-gas from a lab-scale furnace but were unable to determine contributions of each gas to the mass losses [21-23].

In this paper we illustrate the correlation between the gases detected by the GC-MS and the mass loss rate from TGA to obtain a quantitative analysis of contributions of individual gases to mass losses associated with the feed-to-glass conversion and its correspondence to the DSC-TGA results.

THEORY

Although the details of cold-cap reactions are rather complicated, we represent individual reactions with an n^{th}-order kinetic model along with the Arrhenius rate coefficient [7]:

$$\frac{d\alpha_i}{dt} = A_i(1-\alpha_i)^{n_i} \exp\left(-\frac{E_i}{RT}\right) \qquad (1)$$

where α_i is the i^{th} reaction conversion degree, A_i is the i^{th} reaction pre-exponential factor, E_i is the i^{th} reaction activation energy, n_i is the i^{th} reaction apparent order, T is the temperature, and R is the gas constant. Assuming that the reactions are mutually independent, we represent the overall reaction rate as a weighted sum of the rates of individual reactions:

$$\frac{d\alpha}{dt} = \sum_{i=1}^{N} w_i \frac{d\alpha_i}{dt} = \sum_{i=1}^{N} w_i A_i(1-\alpha_i)^{n_i} \exp\left(-\frac{E_i}{RT}\right) \qquad (2)$$

where α is the overall degree of conversion, N is the number of reactions, and w_i denotes the i^{th} reaction fraction such that $\sum_{i=1}^{N} w_i = 1$.

According to Kissinger [24], E_i can be estimated by determining the temperature of the i^{th} peak maximum, T_{im}, for experiments carried out at different heating rates, $\beta \equiv dT/dt$, using the formula

$$\frac{E_i}{R} = -\frac{d(\ln(\beta / T_{im}^2))}{d(1/T_{im})} \tag{3}$$

Pokorný et al. [7] showed that this formula can be applied to gas-evolving cold-cap reactions. The remaining coefficients (A_i, n_i, and w_i) were determined using the least squares optimization..

With ongoing reactions, the DSC essentially measures the total heat flow to the sample from two contributions concurrently: the heat flow associated with the heat capacity of the sample and the heat flow associated with heat of reactions. The simultaneous DSC-TGA measures the total specific heat flow, Q, which, when divided by the rate of heating, attains the heat capacity unit, i.e., heat per unit mass and temperature. Thus, it becomes an "apparent" heat capacity, $c_p^{\text{app}} = Q/\beta$ which comprises heat capacity of the sample, c_p, and the heat generated/consumed by the reactions:

$$c_p^{\text{app}} = c_p + \Delta H \partial_T \alpha \tag{4}$$

where ΔH is the overall specific reaction enthalpy [25]. Note that, although DSC (or simultaneous DSC-TGA) is not the best technique for measuring heat capacities accurately, it can provide an estimate for heat capacity under appropriate experimental conditions (e.g., $\beta \geq$ 10 K min^{-1}) [25,26]. This allowed use of the total heat flows from the simultaneous DSC-TGA in order to obtain, by Equations (2)–(6), the kinetic parameters for individual peaks, as well as ΔH and estimated c_p. To this end, the run/rerun technique and the least square methods were used.

Assuming that the mass loss of the batch is only associated with gas evolution reactions [7] the mass of the feed batch at time t is

$$m(t) = m_i - m_{loss}(t) = m_i - \sum_{j=1}^{N_g} m_j(t) \tag{5}$$

where m_i is the initial mass, m_{loss} is the mass loss, m_j is the mass loss associated with the jth off-gas, and N_g is the number of gas species. Differentiating Eq. (6) with respect to time yields

$$-\frac{\mathrm{d}m(t)}{\mathrm{d}t} = \sum_{j=1}^{N_g} \frac{\mathrm{d}m_j(t)}{\mathrm{d}t} \tag{6}$$

For analysis with GC-MS, the flux of each gas species, represented via abundance, is proportional to the number of molecular ions (or instrumentally induced charges or produced current). Provided that instrumental artifacts are negligible, quantitative analysis can be

established by assuming that the mass change rate of the *j*th off-gas is linearly proportional to the *j*th off-gas abundance or intensity, I_j. Thus,

$$\frac{\mathrm{d}m_j(t)}{\mathrm{d}t} = F_j I_j(t+\Delta t) \tag{7}$$

where F_j is the *j*th off-gas calibration coefficient; F_j is dimensionless such that $F_j I_j$ has an appropriate mass/(time)^2 unit. Here Δt represents a time lag, assumed to be invariant over time or temperature, between the TGA signal and the MS detector reading, due to the off-gas transfer to the MS detector. Inserting Eq. (7) into Eq. (6), one obtains

$$-\frac{\mathrm{d}m(t)}{\mathrm{d}t} = \sum_{j=1}^{N_g} F_j I_j(t+\Delta t) \tag{8}$$

Eq. (8) correlates the mass loss rate, $\mathrm{d}m(t)/\mathrm{d}t$, from TGA, with the I_j from MS via N_g calibration coefficients, which can be obtained using the least squares method.

Under ideal experimental conditions, similar to calibrations performed for quantitative and semi-quantitative MS analyses shown elsewhere [28], a *j*th calibration coefficient can be established by comparing the integrated intensity with the mass change of a solid sample that releases the *j*th gas in a single reaction. Accordingly,

$$\Delta m_j = C_j \int I_j(t)dt \tag{9}$$

where C_j is the *j*th gas calibration coefficient and Δm_j is the mass change of the solid sample during the gas-evolving process. The range of integration is determined by the start and end of the gas-evolving reaction that generates the gas.

EXPERIMENTAL

A simulated high-alumina melter feed (A0), with composition as shown in Table I, was used in this study. The feed was formulated to vitrify a high-alumina HLW to produce glass with the following composition in mass fractions: SiO_2 (0.305), Al_2O_3 (0.240), B_2O_3 (0.152), Na_2O (0.096), CaO (0.061), Fe_2O_3(0.059), Li_2O (0.036), Bi_2O_3 (0.011), P_2O_5 (0.011), F (0.007), Cr_2O_3 (0.005), PbO (0.004), NiO (0.004), ZrO_2 (0.004), SO_3 (0.002), K_2O (0.001), MgO (0.001), and ZnO (0.001) [7,21,27,31]. This glass was designed for the Hanford Tank Waste Treatment and Immobilization Plant, currently under construction at the Hanford Site in Washington State, USA [32]. The batch was heated and stirred at a constant rate to 60 to 80°C, and dried overnight at 105°C, as described elsewhere [27].

TABLE I. Melter feed composition of glass A0

Chemicals	Mass(g)
$Al(OH)_3$	367.49
H_3BO_3	269.83
CaO	60.79
$Fe(OH)_3$	73.82
Li_2CO_3	88.30
$Mg(OH)_2$	1.69
NaOH	99.41
SiO_2	305.05
$Zn(NO_3)_2{\cdot}4H_2O$	2.67
$Zr(OH)_4{\cdot}0.65H_2O$	5.49
Na_2SO_4	3.55
$Bi(OH)_3$	12.80
Na_2CrO_4	11.13
KNO_3	3.04
$NiCO_3$	6.36
$Pb(NO_3)_2$	6.08
$Fe(H_2PO_2)_3$	12.42
NaF	14.78
$NaNO_2$	3.37
$Na_2C_2O_4$	1.26
Total	1349.32

For DSC-TGA, batch samples of 10–60 mg were placed into a Pt crucible of the TA Instruments SDT-Q600 (New Castle, DE, USA) and heated from ambient temperature (~25°C) to 1200°C. The A0 feed was heated at 10°C min^{-1}. The data were expressed in terms of the cumulative mass loss, *x*, and the rate of change, *dx/dT* or *dx/dt*. The T_{im} was determined as a maximum on the *dx/dT* curve; T_ms were estimated for shoulders on larger peaks [21].

For TGA-GC-MS, 61.7 mg of the feed in a Pt crucible were analyzed with a NETZSCH STA 449 F1 Jupiter®[1] - Simultaneous TGA-DSC coupled to GC-MS (Agilent 7890A gas chromatograph equipped with an Agilent 5975C quadrupole MS) via a heated transfer line (200°C). The feed was heated at 10°C min^{-1} from 50°C to 1200°C. Evolved gases move directly from the TGA chamber (under atmospheric pressure) to the GC-MS. Filled evolved gases in the GC were sampled every minute, injected into the GC column, eluted with helium gas, and then reached the MS detector. To avoid condensation, the heated transfer line, the GC column (He with a flow rate of 1.5 mL min^{-1}), and the connecting valve were all kept at 200°C. MS ionization energy was set to 20 eV and the scan range *m*/*z* (mass-to-charge ratio) set from 10–100. The reproducibility was checked at the optimized setting conditions (i.e., temperature, size of crucible, and flow rates specified) over multiple times. The National Institute of Standards and Technology (NIST) mass spectral database, containing a collection of electron ionization mass spectra for various molecular species, was employed to identify evolved gases.

[1] Jupiter is a registered trademark of Netzsch Geratebau GMBH.

RESULTS

TGA-GC-MS Results of $CaCO_3$

The thermal decomposition of calcium carbonate has been intensively studied due to its wide industrial application and the apparent simplicity of the reaction. The Calcium carbonate decomposition reaction involves a relatively large mass loss associated with CO_2 evolution according to the reaction [29].

$$CaCO_3(s) \rightarrow CaO(s) + CO_2\,(g) \qquad (10)$$

This compound is an appropriate reference for the TGA-GC-MS system because its decomposition stoichiometry is well known, the product is not hygroscopic, and the decomposition steps are distinct and well resolved [30]. The TGA experiment was completed by heating 6.5 mg $CaCO_3$ at 10°C min^{-1} from 50°C to 1200°C in a 20-ml min^{-1} helium flow. The evolved gases were analyzed using GC-MS. After chromatographic separation, the evolved gas, CO_2, was identified by its mass spectra through the interactive library search. The measured $CaCO_3$ weight loss of 43.20% compares well with the stoichiometric weight loss of 43.96%. Because of the instrument configuration and GC column, a lag time was considered to adjust the MS curve and TG mass loss. The MS and normalized weight derivative (DTG) plots are combined in Fig. 1 and show that $CaCO_3$ thermal decomposition takes place between 530°C and 775°C.

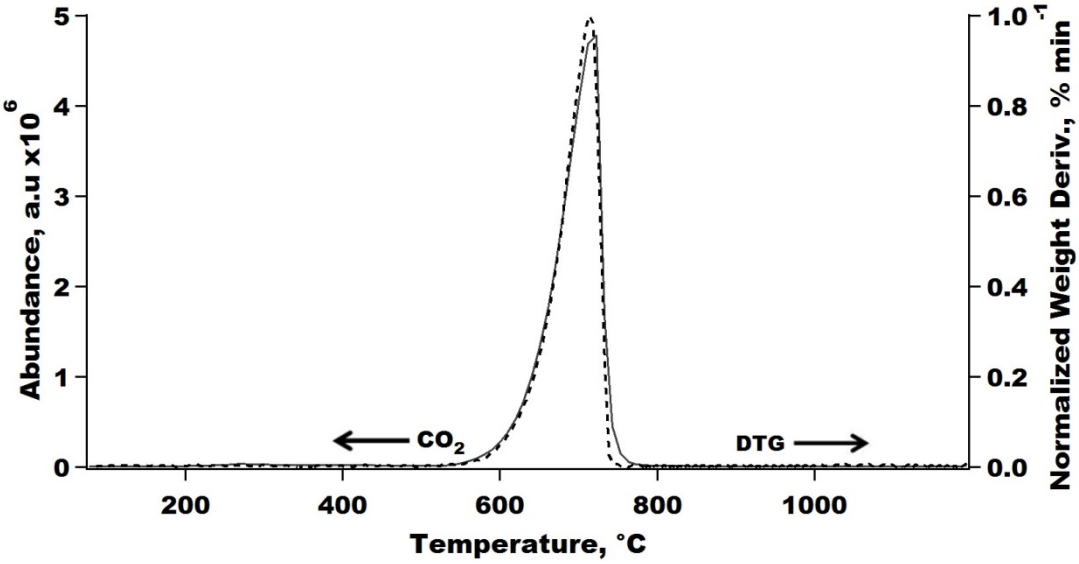

Figure 1. TGA-MS (*m*/*z* = 44) (solid line) and DTG (dotted line) curves of $CaCO_3$ decomposition at 10°C min^{-1} heating rate

DSC-TGA Results of A0 Simulated High Alumina Feed

DSC-TGA activation energies with corresponding coefficients, values of log(A_i/s^{-1}) with averages, values of w_i with averages, optimized w_i values with averaged log(A_i/s^{-1}) values and their correspondent standard deviations (Stdev), and relative standard deviation (RSD) for peaks 1–8 and four heating rates (β) were obtained elsewhere [21].]. Fig. 2 shows measured (solid lines) and fitted (dashed lines) overall reaction rates, along with individual reaction peaks, based on the averaged values of log (A_i /s^{-1}) and averages of selected values of n_i. The results of the least squares analyisis for eight major reactions and agreement between the measured and fitted curve are satisfactory [21].

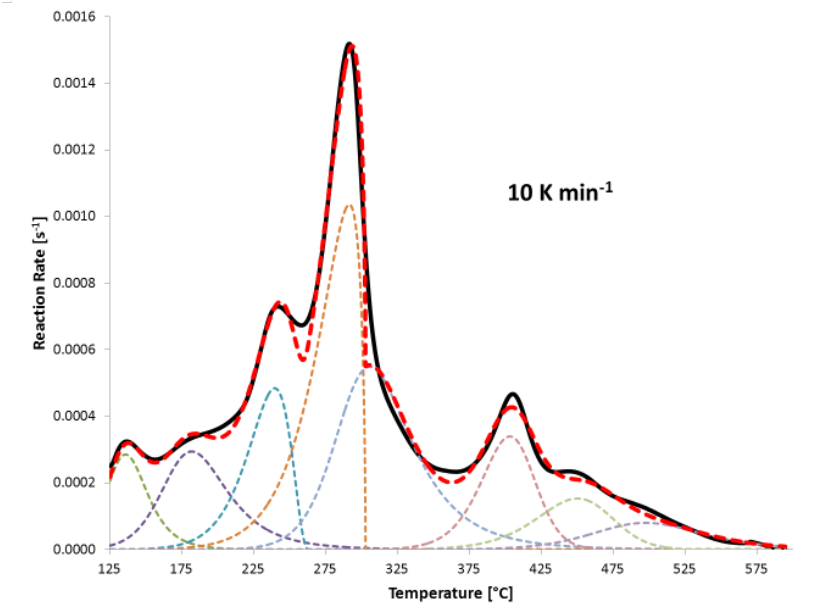

Figure 2. Measured and fitted TGA- DSC peaks

Fig. 3 shows a comparison between the DSC (solid line) and TGA (dashed line) curves for 10 K min^{-1}. The TGA response [7] was multiplied by 5 because $\sum_{i=1}^{N} w_i^{TGA} = 0.20$ whereas $\sum_{i=1}^{N} w_i^{DSC} = 1$. The numbers represent the DSC peaks (Fig.2).

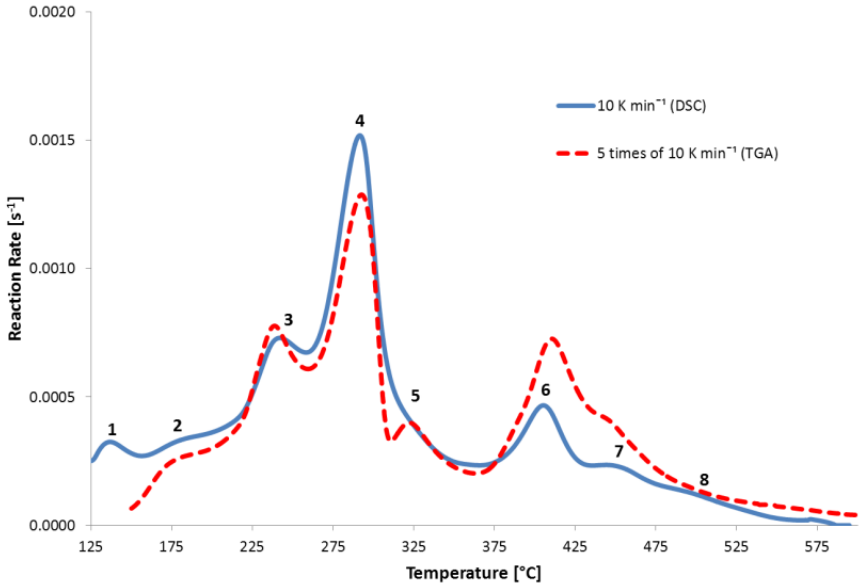

Figure 3. TGA-DSC reaction rate data comparison

TGA-GC-MS Results of A0 Simulated High Alumina Feed

Figure 4 shows TGA normalized weight and normalized weight derivative (DTG) of A0 feed heated at 10 K min^{-1}.

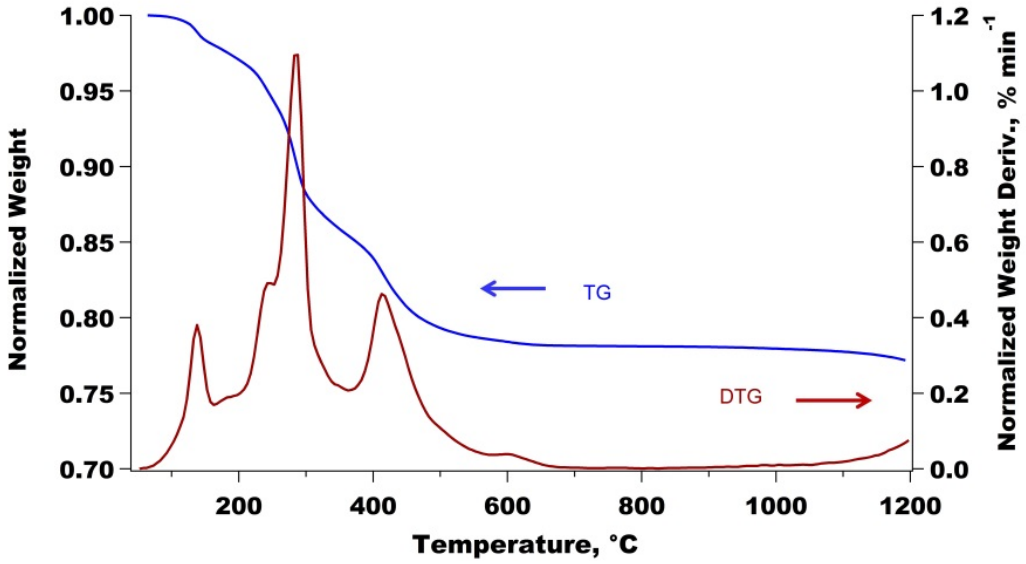

Figure 4. Raw TGA data

Using the NIST database, the gases detected by the MS (see Fig. 5) were identified by their decomposition masses: m/z = 44 for CO_2, 18 for H_2O, 30 for NO, and 32 for O_2. The major gases were CO_2 and H_2O. The generation of O_2 was appreciable only at $T \geq 900$°C. The minor NO peak coincides with the major peak of CO_2.

To match the DTG and GC-MS temperature scales, data were smoothed with spline interpolation and a ~1.5-min time lag was applied. The time lag of the off-gas transfer from the TGA to the MS detector corresponds to the 1.5-mL min^{-1} flow rate through the 30-m column with an inner diameter of 320 μm.

Calibration coefficients (F_j) (Table II) were obtained using least squares analysis. To resolve the issue of overlapped CO_2 and NO peaks, the least squares optimization was constrained using the NO/CO_2 ratio of 0.0732 based on the content of carbon and nitrogen in the feed. The difficulty of quantifying the O_2 release was bypassed by applying separate least squares analyses to $T < 690$°C for H_2O and CO_2 and $T > 690$°C for O_2.

Table II. Calibration coefficients for individual evolved gases

Gas	Calibration coefficient
H_2O	1.15×10^{-6}
CO_2	1.36×10^{-7}
NO	2.98×10^{-7}
O_2	7.20×10^{-8}

Fig. 5 compares the mass change rates from DTG with GC-MS gas evolution rates obtained with the F_j values listed in Table II. The EGA curve in Fig. 5 represents total gas evolution rate. The good agreement between DTG and EGA demonstrates that Eq.(7) yields a reasonable simulation.

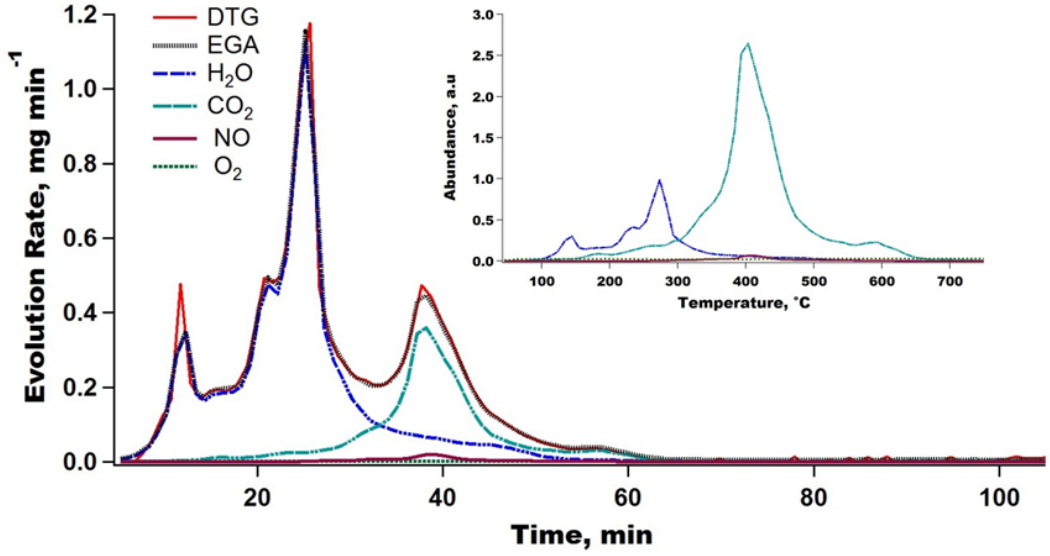

Figure 5. GC-MS spectra and gas evolution rates for gaseous species by TGA and GC-MS of A0 feed heated at 10 K min^{-1}

DISCUSSION

The previously reported TGA analysis [7] was solely focused on reaction kinetics. Identifying the gases by EGA provides a step toward the identification of the gas-evolving reactions for individual TGA peaks with the ultimate goal of understanding the reaction mechanisms. As Fig. 5 shows, the TGA peaks for individual gases overlap. By EGA results, the TGA peaks below 400°C mainly correspond to H_2O evolution and the TGA peaks above 400°C correspond to CO_2, NO and O_2 evolution (see Fig. 6). While the EGA can add the chemical characteristics to the peaks identified in the TGA, it cannot differentiate detailed individual reactions to produce the same gas. The identification of individual reactions and a more precise quantification of each evolved gas requires additional information and tests. Figure 6 compares the reaction rates from the TGA-DSC–based analysis and the scaled calibration approach from TGA-GC-MS.

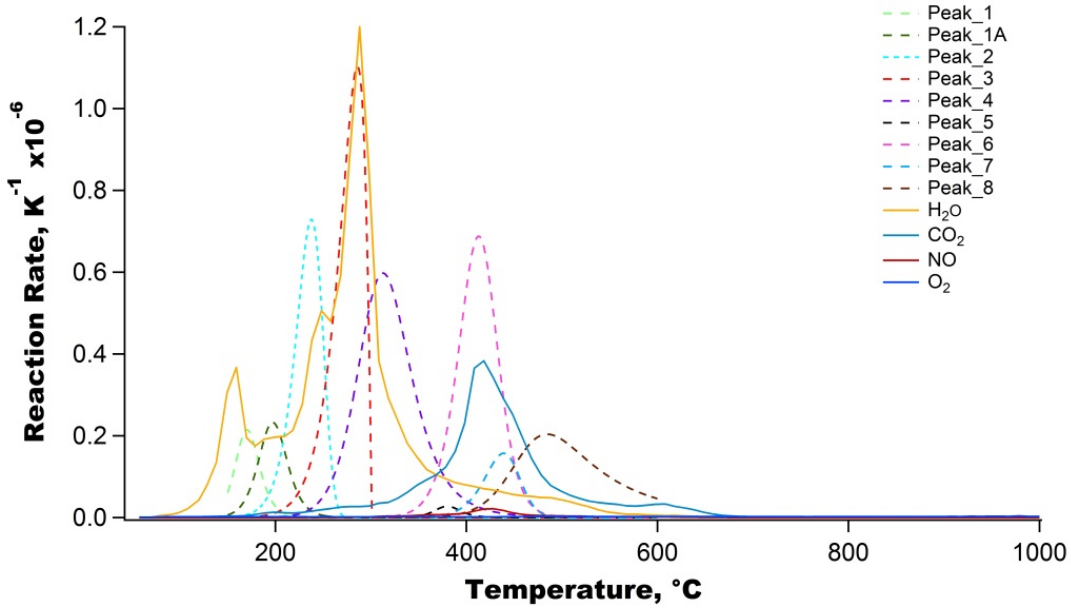

Figure 6. Reaction rates from the TGA-DSC–based analysis and the scaled calibration approach from TGA-GC-MS.

CONCLUSIONS

The DSC-TGA and TGA-GC-MS have shown to be good experimental tools for EGA. The TGA-GC-MS analysis identifies gases evolved from melter feeds during their conversion to molten glass. A simple calibration approach correlates the mass loss rate from TGA to the production rate of individual gases from EGA on a quantitative basis. This identifies where specific mass loss occurs as melter feed is heated and goes through various reactions and releases CO_2, H_2O, NO, and O_2. A detailed evolved gas analysis provides a key element to a more complete understanding of the cold cap reactions.

REFERENCES

1. P. Hrma, Melting of Foaming Batches: Nuclear Waste Glass, *Glastech. Ber.* 63K:360 (1990).
2. P. Hrma, J. Matyáš, and D-S Kim, The Chemistry and Physics of Melter Cold Cap, In: *9th Biennial Int. Conf. on Nucl. and Hazardous Waste Management, Spectrum '02*, American Nuclear Society, La Grange Park, IL (2002).
3. D.F. Bickford, P. Hrma, and B.W. Bowen, II, Control of Radioactive Waste Glass Melters: II, Residence Time and Melt Rate Limitations, *J. Amer. Ceram. Soc.* **73**,2903 (1990)
4. D. Kim, M.J. Schweiger, W.C. Buchmiller, and J. Matyas, Laboratory-Scale Melter for Determination of Melting Rate of Waste Glass Feeds PNNL-21005, Pacific Northwest National Laboratory, Richland, Washington (2012).
5. R. Pokorný and P. Hrma, Mathematical modeling of cold cap, *J. Nucl. Mater.* **429**, 245–256 (2012).
6. P. Hrma, A.A. Kruger, and R. Pokorný, Nuclear waste vitrification efficiency: cold cap reactions, *J. Non-Cryst. Solids*, **358,** 3559–3562 (2012).
7. R. Pokorný, D.A. Pierce, and P. Hrma, Melting of glass batch: Model for multiple overlapping gas-evolving reactions, *Thermochim. Acta* **541**, 8–14 (2012).
8. F.W. Wilburn and C.V. Thomasson, The application of differential thermal analysis and thermogravimetric analysis to the study of reactions between glass-making materials. Part 1. The sodium carbonate–silica system, *J. Soc. Glass Technol.* **42,** 158T–175T (1958).
9. C.V. Thomasson and F.W. Wilburn, The application of differential thermal analysis and thermogravimetric analysis to the study of reactions between glass-making materials. Part 2. The calcium carbonate–silica system with minor batch additions, *Phys. Chem. Glasses* **1**, 52–69 (1960).
10. F.W. Wilburn and C.V. Thomason, The application of differential thermal analysis and thermogravimetric analysis to the study of reactions between glass-making materials. Part 3. The sodium carbonate–silica system, *Phys. Chem. Glasses* **2**, 126–131 (1961).
11. F.W. Wilburn and C.V. Thomason, The application of differential thermal analysis and differential thermogravimetric analysis to the study of reactions between glass-making materials. Part 4. The sodium carbonate–silica–alumina system, *Phys. Chem. Glasses* **4**, 91–98 (1963).
12. F.W. Wilburn, S.A. Metcalf, and R.S. Warburton, Differential thermal analysis, differential thermogravimetric analysis, and high temperature microscopy of reactions between major components of sheet glass batch, *Glass Technol*. **6**, 107–114 (1965).
13. E. Bader, Thermoanalytical investigation of melting and fining of Thüringen laboratory glassware, *Silikattechnik* **29**, 84–87 (1978).
14. J. Mukerji, A.K. Nandi, and K.D. Sharma, Reaction in container glass batch, *Ceram. Bull*. **22**, 790–793 (1979).
15. O. Abe, T. Utsunomiya, and Y. Hoshino, The reaction of sodium nitrate with silica, *Bull. Chem. Soc. Jpn*. **56**, 428–433 (1983).
16. T.D. Taylor and K.C. Rowan, Melting reactions of soda-lime-silicate glasses containing sodium sulfate, *J. Am. Ceram. Soc*. **66**, C227–228 (1983).
17. M. Lindig, E. Gehrmann, and G.H. Frischat, Melting behavior in the system SiO2-K2CO3-CaMg(CO3)2 and SiO2-K2CO3-PbO, *Glastech. Ber*. **58**, 27–32 (1985).
18. C.A. Sheckler and D.R. Dinger, Effect of particle size distribution on the melting of soda-lime-silica glass, *J. Am. Ceram. Soc.* **73**, (1990) 24–30 (1990).

19. K.S. Hong and R.E. Speyer, Thermal analysis of reactions in soda-lime-silicate glass batches containing melting accelerants: I. One- and two-component systems, *J. Am. Ceram. Soc*. **76**, 598–604 (1993).
20. K.S. Hong, S.W. Lee, and R.E. Speyer, Thermal analysis of reactions in soda-lime-silicate glass batches containing melting accelerants: II. Multicomponent systems, *J. Am. Ceram. Soc*. **76**, 605–608 (1993).
21. J. Chun, D.A. Pierce, R. Pokorný, and P. Hrma, Cold-cap reactions in vitrification of nuclear waste glass: experiments and modeling. Thermochim. Acta 559 (2013) 32–39.
22. P.A. Smith, J.D. Vienna, and P. Hrma, The effects of melting reactions on laboratory-scale waste vitrification. *J. Mater. Res*. **10**, 2137–2149 (1995).
23. J. Matyáš, P. Hrma, and D.-S. Kim, Melt Rate Improvement for High-Level Waste Glass, PNNL-14003, Pacific Northwest National Laboratory, Richland, Washington, (2002).
24. H. E Kissinger, Reaction kinetics in differential thermal analysis ,Anal.Chem.29 (1957)204-237.
25. M Reading, A. Luget, R. Wilson, Modulated differential scanning calorimetry, Thermohim, Acta 238 (1994) 295-307.
26. M.J. O'Neill, Measurement of specific heat functions by differential scanning calorimetry, Anal. Chem. 38 (1966) 1331–1336.
27. M.J. Schweiger, P. Hrma, C.J. Humrickhouse, J. Marcial, B.J. Riley, and N.E. TeGrotenhuis, Cluster formation of silica particles in glass batches during melting, *J. Non-Cryst. Solids* **356**, 1359–1367 (2010).
28. P.R. Hrma, M.J. Schweiger, B.27M. Arrigoni, C.J. Humrickhouse, J. Marcial, A. Moody, C. Rodriguez, R.M. Tate, and B. Tincher, Effect of Melter-Feed-Makeup on Vitrification Process, PNNL-18374, Pacific Northwest National Laboratory, Richland, Washington, (2009).
29. Velyana Georgieva, Lyubomir Vlaev, and Kalinka Gyurova, "Non-Isothermal Degradation Kinetics of $CaCO_3$ from Different Origin," Journal of Chemistry, vol. 2013, Article ID 872981, 12 pages, 2013. doi:10.1155/2013/872981
30. M. Maciejewski, C.A. Müller, R. Tschan, W.D. Emmerich, and A. Baiker, *Thermochim. Acta*, **295**, 167 (1997).
31. D. R. DIXON, M. J. SCHWEIGER, P. HRMA, "Effect of Feeding Rate on the Cold Cap Configuration in a Laboratory-Scale Melter," WM2013 Conference, Paper#13362, Phoenix, AZ (2013).

ACKNOWLEDGEMENTS

This work was supported by the Department of Energy's Waste Treatment & Immobilization Plant Federal Project Office under the direction of Dr. Albert Kruger. The authors are grateful to Drs. Dong-Sang Kim and Ekkehard Post for insightful discussions and instructions on the TGA-GC-MS setup and tests, respectively. Pacific Northwest National Laboratory is operated by Battelle Memorial Institute for the U.S. Department of Energy under contract DE-AC05-76RL01830.